

**Spectroscopic Investigations of Mare Basalts within Imbrium Basin Using M<sup>3</sup> Data.** F. Zhang<sup>1,2</sup>, Y. L. Zou<sup>1</sup>, Y. C. Zheng<sup>1</sup>, X. H. Fu<sup>1</sup>, and Y.C. Zhu<sup>1,2</sup> <sup>1</sup>National Astronomical Observatories, CAS, Beijing, A20 Datun Road, Chaoyang District, Beijing 100012, P.R. China, <sup>2</sup> University of CAS, Beijing, A19 Yuquan Road, Shijingshan District, Beijing, 100049. (fzhang@nao.cas.cn)

**Introduction:** The surface of our nearest neighbor-Moon preserves a record of igneous activity dating back to early in the thermal evolution history of the solar system. For many years, the second largest basaltic region of Mare Imbrium (after Oceanus Procellerum) has been an important target of geologic investigation [1, 2, 3] for its important role in the chronology framework of the Moon unraveled by several giant and typical impacting events, which caused extensive mare filling. Previous studies of younger western maria using high spatial resolution Clementine UVVIS and NIR data [4, 5] and higher spatial and spectral resolution Moon Mineralogical Mapper (M<sup>3</sup>) data [6] examined fresh mare craters and associated soils within Imbrium flows. These studies determined that the strong and asymmetric 1000 nm absorptions within mare soils and relatively weak 2000 nm ferrous absorptions were also present for crystalline materials excavated from varying depths throughout these flows by optically immature craters. Within Mare Imbrium (Fig.1), the basaltic flows flood small and large Eratosthenian craters and cover older Imbrian deposits, providing a context for their stratigraphic age [7].

We aim to have an investigation on the diagnostic reflectance properties of individual flows within these basalts, which can be measured by M<sup>3</sup> data and provide the observations necessary for detailed interpretation of their mineralogy and petrologic evolution.

**Data:** Moon Mineralogical Mapper (M<sup>3</sup>), is a push broom hyperspectral sensor on board India's Chandrayaan 1 mission. It operates in the spectral range 0.46-3.0 μm [8]. The M<sup>3</sup> visible to infrared reflectance data at spatial and spectral resolutions is capable of measuring discrete basaltic flows within the lunar maria [9]. For this study, a large mosaic of global mode M<sup>3</sup> data has been created at its full spectral and spatial resolution using 54 orbits of data from optical period 1B. This radiometrically calibrated data, which is the level 2 reflectance data products that were derived from the level 1B reflectance data products, covers the wavelength range of ~0.43 to 3.0 μm in 85 spectral bands at a spatial resolution of 140 m/pixel from 100 km orbit. Details about M<sup>3</sup> data acquisition and radiometric calibration are discussed in detail by [10].

**Method:** The strength of absorption bands is one of the diagnostic parameters of VIS-NIR reflectance spectra related to a mineral's crystal structure and Fe abundance and it can be measured as the band depth at the band center [11]. The band depth parameter is not

only dependent on the chemical composition of a material but is also affected by the presence of strongly absorbing opaque minerals (such as ilmenite), the effects of space weathering, and observational conditions [12, 13, 14]. The band depth ( $D_H$ ) is computed using the equation [15] as follows:

$$D_H = 1 - R_B / R_C$$

Where  $R_B$  is the reflectance at the band center and  $R_C$  is the reflectance of the continuum at the band center. The continuum of a VIS-NIR spectrum is defined as a convex hull to the reflectance spectrum.

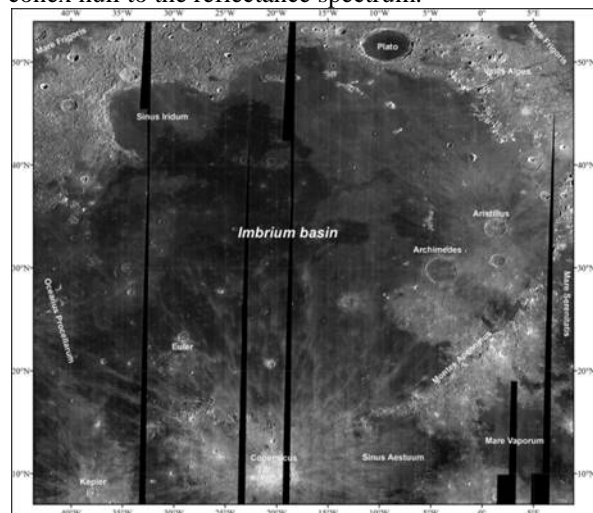


**Figure 1:** Eratosthenian age mare deposits in the Imbrium basin appear dark at 1.27 μm in this M<sup>3</sup> mosaic.

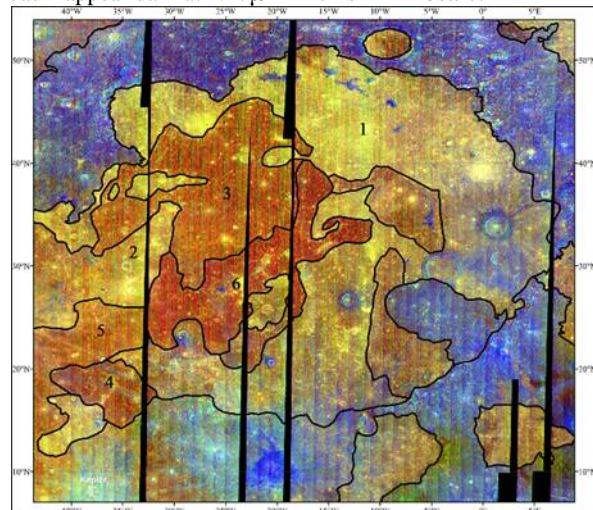


**Figure 2:** Late stage lunar volcanism within the Imbrium basin appears as a distinct red hue in this M<sup>3</sup> color composite (ref for 1 μm IBD, green for 2 μm IBD, blue for reflectance at 1.58 μm).

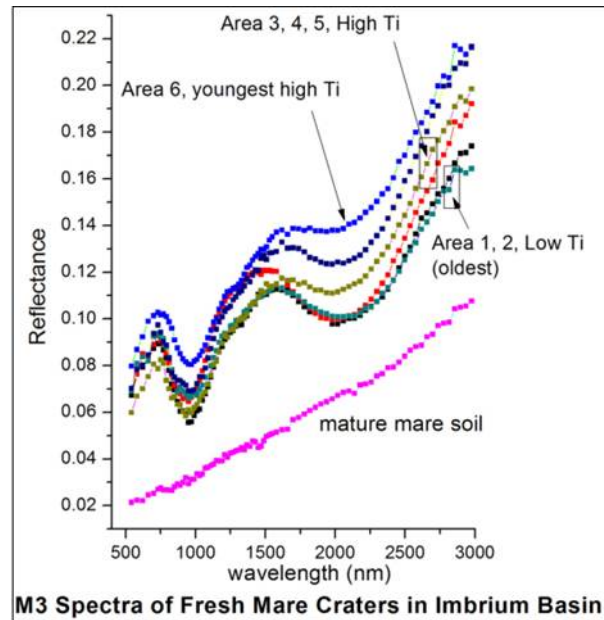
Absorption features centred around 1000 nm and 2000 nm are important for the study of mafic mineral such as olivine and pyroxenes on Moon. The iron-bearing minerals, pyroxene and olivine have strong absorption near 1000 nm and the former is having additional feature around 2000 nm. The spinel has characteristic absorption near 2000 nm. The integrated band (IBD) depth 1000 and 2000 nm region will tell about the presence of the minerals as well as their relative abundance. Higher the IBD value, higher the concentration of the mineral present. The non iron-bearing minerals such as plagioclase, silica will not have any spectral feature in this region. In the present study, we aim to use this nature of IBD to distinguish mare units in Imbrium basin.

M<sup>3</sup> science team has used these two parameters, 1000 nm IBD and 2000 nm IBD for bringing out the lithological diversity of lunar surface [e.g., 6, 16, 17]. In case of 1000 IBD, a line connecting the 789 nm and 1308 nm defines the continuum and in the case of the 2000 IBD; a line joining 1658 and 2498 nm defines continuum. The color composite (Fig.2) created by assigning red to 1000 nm IBD, green to 2000 nm IBD and blue to Albedo of 1548 nm band is an excellent tool to discriminate between diverse lunar lithology.

#### Data Analysis:

Basaltic deposit spectra (Fig.3) exhibit that crater materials from the high-Ti flows display a broader and longer wavelength absorptions at 1 $\mu$ m and weaker absorptions at 2  $\mu$ m than the surrounding low titanium basalts. Spectra from the youngest flow unit (area 6) exhibits slightly longer wavelength absorptions than the earlier high-Ti basalts (area 3, 4, and 5). These initial results are consistent with a potential increase in olivine content in the uppermost flows. Many craters in the high-Ti deposits of Imbrium exhibit 1 and 2  $\mu$ m absorptions that are more typical of pyroxene-rich basalts.

**Discussion and Future Work:** A sample of the M<sup>3</sup> data spectra derived from optically immature craters in each mare region is presented in Figure 3. In this work, we continue the preliminary investigations by [18] to examine the mineralogical composition of the basaltic flows. Comparing with low-Ti basalts, crater materials from the high-Ti flows exhibit a broader and longer wavelength absorptions at 1 $\mu$ m and weaker absorptions at 2 $\mu$ m than the surrounding low-Ti basalts. Spectra from the youngest flow unit (phase 3) displays slightly longer wavelength absorptions than the earlier high-Ti basalts (phase 1). Again, these initial results are consistent with a potential increase in olivine content in the upper most flows [e.g., 4, 18].



**M<sup>3</sup> Spectra of Fresh Mare Craters in Imbrium Basin**

**Figure 3:** M<sup>3</sup> spectra of relatively unweathered crater materials from various stratigraphic units within Imbrium.

Future work will include detailed mapping of visible flows for correlation with M<sup>3</sup> spectral units and crater age maps. High resolution images from the LRO and CE-2 missions will be used along with the M<sup>3</sup> data for mapping and examination of potential source features.

Our work will also have integrated in-depth analysis of diverse mare regions of microwave brightness temperature variations with the data [19] acquired by the microwave radiometer (MRM), one of the eight scientific instruments on board the spacecraft Chang'E-1.

#### References:

- [1] Schaber, G.G. (1973) Apollo 17: Preliminary Science Report, 30/17-25. [2] Moore, H.J. and Schaber, G.G. (1975) PLPSC, 101-118. [3] Spudis, P.D. et al. (1988) PLPSC, 155-168. [4] Staid, M.I. and Pieters, C.M. (2001) JGR 106, 27,887-27,900. [5] Staid, M.I. et al. (2002) PLPSC, abstract 1795. [6] Staid, M.I. et al. (2011) JGR 116, E00G10. [7] Wilhelms, 1987, U.S. Geol. Surv. Prof. Pap. 1348. [8] Pieters, C.M. (2009) Current Science 96, 500-505. [9] Staid, M.I. and Besse, S. (2013) PLPSC, abstract 2661. [10] Boardman, J. et al. (2011) JGR 116, E00G14. [11] Bhatt, M. et al. (2012) Icarus 220, 51-64. [12] Pieters, C.M. et al. (2000) Meteoritics & Planetary Science 35, 1101-1107. [13] Hapke, B. (2001) JGR 106, 10,039-10,074. [14] Noble, S.K. et al. (2007), Icarus 192, 629-642. [15] Clark, R.N. and Roush, T.L. (1984) JGR, 89, 6329-6340. [16] Besse, S. et al. (2011) JGR, 116, E00G13. [17] Mustard, J.F. et al. (2011) JGR 116, E00G12. [18] Staid, M. and Besse, S. (2013) 44<sup>th</sup> PLPSC, abstract 2661. [19] Ouyang, Z.Y. et al. (2010) SCIENCE CHINA Earth Science 53, 1565-1581.